

Multiclustered chimeras in large semiconductor laser arrays with nonlocal interactionsJ. Shena,^{1,2} J. Hizanidis,^{1,2,*} P. Hövel,^{3,4} and G. P. Tsironis^{1,2,5}¹*Crete Center for Quantum Complexity and Nanotechnology, Department of Physics, University of Crete, P. O. Box 2208, 71003 Heraklion, Greece*²*National University of Science and Technology MISiS, Leninsky prosp. 4, Moscow, 119049, Russia*³*Institut für Theoretische Physik, Technische Universität Berlin, Hardenbergstraße 36, 10623 Berlin, Germany*⁴*Bernstein Center for Computational Neuroscience Berlin, Humboldt-Universität zu Berlin, Philippstraße 13, 10115 Berlin, Germany*⁵*School of Engineering and Applied Sciences, Harvard University, Cambridge, Massachusetts 02138, USA*

(Received 5 June 2017; published 18 September 2017)

The dynamics of a large array of coupled semiconductor lasers is studied numerically for a nonlocal coupling scheme. Our focus is on chimera states, a self-organized spatiotemporal pattern of coexisting coherence and incoherence. In laser systems, such states have been previously found for global and nearest-neighbor coupling, mainly in small networks. The technological advantage of large arrays has motivated us to study a system of 200 nonlocally coupled lasers with respect to the emerging collective dynamics. Moreover, the nonlocal nature of the coupling allows us to obtain robust chimera states with multiple (in)coherent domains. The crucial parameters are the coupling strength, the coupling phase and the range of the nonlocal interaction. We find that multiclustered chimera states exist in a wide region of the parameter space and we provide quantitative characterization for the obtained spatiotemporal patterns. By proposing two different experimental setups for the realization of the nonlocal coupling scheme, we are confident that our results can be confirmed in the laboratory.

DOI: [10.1103/PhysRevE.96.032215](https://doi.org/10.1103/PhysRevE.96.032215)**I. INTRODUCTION**

Coupled lasers have been extensively studied in terms of nonlinear dynamics [1–5] and synchronization phenomena [6–8]. Most of these studies have been concerned with semiconductor laser arrays. They have been demonstrated as sources that can produce high output power in a spatially coherent beam. Coupling between lasers may arise due to the overlap of the electric fields from each laser waveguide or due to the presence of an external cavity [9,10]. In the latter case, a time delay is required for the mathematical modeling of the system. In general, most works on laser arrays consider either global coupling, where each laser interacts with the whole system [11,12], or local coupling, where each laser interacts with its nearest neighbors [13,14]. The main property of those systems is that although the emission from the individual elements is often unstable and even chaotic [15], the total light output from the semiconductor array can be stable.

In recent years, semiconductor laser networks have been studied in terms of a peculiar form of synchronization called *chimera states*. Since the first discovery of chimeras for symmetrically coupled Kuramoto oscillators in 2002 [16], this counterintuitive symmetry breaking phenomenon of partially coherent and partially incoherent behavior has received enormous attention (see Ref. [17] and references within). In laser systems, chimeras were first reported both theoretically and experimentally in a virtual space-time representation of a single laser system subject to long delayed feedback [18,19]. Small networks of globally delay-coupled lasers have also been studied and chimera states were found for both small and large delays [10,20]. Moreover, “turbulent” chimeras were recently observed and classified in large arrays of nonidentical laser arrays with nearest-neighbor interactions [21]. There, the

crucial parameters were the coupling strength and the relative optical frequency detuning between the emitters of the array.

The experimental realization of laser arrays is challenging, but these devices have significant technological advantages: By achieving phase locking of the individual lasers we obtain a coherent and high-power optical source. In Ref. [22] synchronization phenomena were studied in large networks with both homogeneous and heterogeneous coupling delay times. Moreover, in Ref. [23] a new experimental approach to observe large-scale geometric frustration with 1500, both nonlocally and locally, coupled lasers was presented. In the present work, we will focus on the intermediate case, i.e., nonlocal coupling. In laser networks this kind of coupling has never been attempted before, and with this paper we aim to fill this gap. In our study we use nonlocal coupling, where the crucial parameters for the observed dynamics are the strength, the phase and the range of the coupling. Our focus, in particular, is to identify the parameter regions where chimera states or other phenomena emerge and subsequently characterize them following a recently proposed classification scheme [24].

II. THE MODEL

In the present analysis, we consider a ring of $M = 200$ semiconductor lasers of class B. Each node j is symmetrically coupled with the same strength to its R neighbors on either side (nonlocal coupling). The evolution of the slowly varying complex amplitudes $\mathcal{E}_j = E_j \exp(i\phi_j)$ (where E_j is the amplitude and ϕ_j the phase of the electric field) and the corresponding population inversions N_j are given by

$$\frac{d\mathcal{E}_j}{dt} = (1 + ia)\mathcal{E}_j N_j + \frac{ke^{-i2C_p}}{2R} \sum_{l=j-R}^{j+R} \mathcal{E}_l, \quad (1a)$$

$$\frac{dN_j}{dt} = \frac{1}{T} [p - N_j - (1 + 2N_j)|\mathcal{E}_j|^2], \quad j = 1, \dots, M, \quad (1b)$$

*hizanidis@physics.uoc.gr

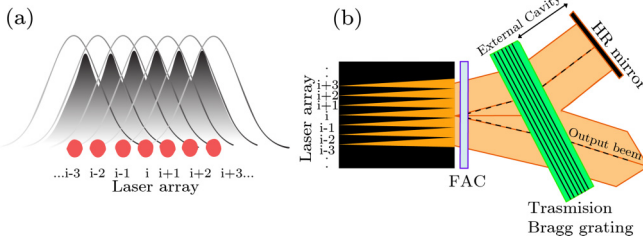


FIG. 1. Conceptual model of (a) the overlap of the electric fields in nonlocally coupled waveguide lasers and (b) a laser array coupled by a common highly reflective (HR) mirror via an external cavity. (FAC denotes fast-axis collimating lens.)

where all indexes has to be taken modulo M . T is the ratio of the lifetime of the electrons in the excited level and that of the photons in the laser cavity. Lasers are pumped electrically with the excess pump rate $p = 0.23$ [10]. The linewidth enhancement factor a models the relation between the amplitude and the phase of the electrical field. We consider $a = 2.5$, which is a typical value for semiconductor lasers. The coupling strength k and the phase C_p are the control parameters that are used to tune the collective dynamics of the system. This complex coupling coefficient models the important effect of a phase shift introduced as the electric field of one laser couples into another [25]. Equations (1) are a reduced form of the Lang-Kobayashi model in the limit where the delay of the external cavity tends to zero [10]. By shifting the coupling phase to $(C_p + \pi)$, we can obtain the model that describes the interaction of each field of semiconductor lasers in an array of waveguides [11,12].

Physically, nonlocal coupling arises due to the overlap of the electric fields within a range of R neighbor waveguides of lasers [see Fig. 1(a)]. In this case, a portion of the electric field from one laser extends into the active region of its $2R$ neighboring lasers. The strength of this field extension decreases in space but for simplicity we assume a uniform coupling k in every active region of $2R$ lasers. Another scheme corresponding to this type of coupling can be achieved by replacing all waveguides by a single external cavity where the length of it or the delay tends to zero [see Fig. 1(b)]. In that case the converging lense coupler for all of lasers inside the cavity cannot converge all the M beams of light in one beam and so a nonlocal coupling is a more realistic approach than an all-to-all coupling. Equations (1) are numerically integrated using a fourth-order Runge-Kutta algorithm with a fixed time step and periodic boundary conditions. For the initial conditions, the phases of the individual lasers are randomly distributed along the complex unit circle while amplitudes and inversions are chosen identical for all lasers $E_j(t = 0) = \sqrt{p}$, $N_j(t = 0) = 0$. Moreover, the well known period $T_r = 2\pi/\Omega$ of the individual laser relaxation oscillation frequency $\Omega = \sqrt{2p/T}$ will set the time scale of the system. For the parameters considered in this work, we obtain $T_r \simeq 183$. This high value of T_r has motivated us to neglect the delay term τ in the coupling for simplicity, since we obtain similar results for $\tau \leq 1$. In order to understand the effect of all three control parameters, namely the coupling strength k , the coupling range R and the coupling phase C_p , we split the problem into two parts: In the first part, the coupling phase is set to zero and the coaction

of the coupling strength and range is studied. In the second part, the coupling phase is also considered and we will show that more complex phenomena like chimera states emerge. In the concluding section, we summarize our results and discuss open problems.

III. MEASURES FOR PHASE AND AMPLITUDE SYNCHRONIZATION

By using polar coordinates the characterization of the phase synchronization of our system can be done through the Kuramoto local order parameter [26]:

$$Z_j = \left| \frac{1}{2\zeta} \sum_{|l-j| \leq \zeta} e^{i\phi_l} \right|. \quad (2)$$

We use a spatial average with a window size of $\zeta = 3$ elements. A Z_j value close to unity indicates that the j th laser belongs to the coherent regime, whereas Z_j is closer to 0 in the incoherent part. This quantity can measure only the phase coherence and gives no information about the amplitude synchronization of the electric field. For the latter, we will use the classification scheme presented in Ref. [24] for spatial coherence, which we have applied to other systems in recent works as well [21,27]. In particular, we will calculate the so-called *local curvature* at each time instance, by applying the absolute value of the discrete Laplacian $|DE|$ on the spatial data of the amplitude of the electric field:

$$|DE|_j(t) = |E_{j+1}(t) - 2E_j(t) + E_{j-1}(t)|, \quad j = 1, \dots, M. \quad (3)$$

In the synchronization regime the local curvature is close to zero while in the asynchronous regime it is finite and fluctuating. Therefore, if g is the normalized probability density function of $|DE|$, then $g(|DE| = 0)$ measures the relative size of spatially coherent regions in time. For a fully synchronized system $g(|DE| = 0) = 1$, while for a totally incoherent system it holds that $g(|DE| = 0) = 0$. A value between 0 and 1 of $g(|DE| = 0)$ indicates coexistence of synchronous and asynchronous lasers.

Note that the quantity g is time dependent. Complementary to the local curvature we also calculate the spatial extent occupied by the coherent lasers which is given by the following integral:

$$g_0(t) = \int_0^\delta g(t, |DE|) d|DE|, \quad (4)$$

where $\delta = 0.001$ is a threshold value distinguishing between coherence and incoherence, which is related to the system-dependent, maximum curvature.

IV. COLLECTIVE DYNAMICS

In Fig. 2(a), the temporal mean of $g_0(t)$, averaged over $100T_r$, is plotted in the (R, k) parameter space. There are four distinct regions: The blue area corresponds to the unsynchronized region, where $g_0(t)$ is close to zero and is denoted by **I**, and the red region, denoted by **IV**, refers to a stationary state where all lasers enter a fixed point and therefore

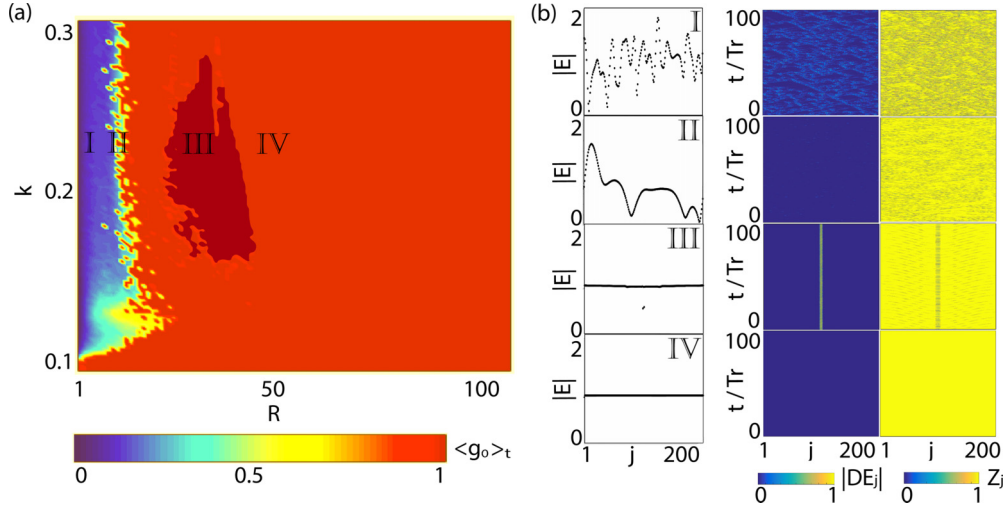


FIG. 2. (a) Dependence of the temporal mean $\langle g_0(t) \rangle$ on parameters k and R . (b) Snapshot of the amplitude of the electric field (left), spatiotemporal evolution of the local curvature (middle), and the local order parameter (right) for fixed $k = 0.21$ and four different coupling ranges: (I) $R = 2$, (II) $R = 9$, (III) $R = 29$, and (IV) $R = 50$. Other parameters: $T = 392$, $p = 0.23$, $a = 2.5$, and $C_p = 0$.

$g_0(t)$ is close to unity. Apart from those two well defined regions, there exist two more interesting ones for intermediate values of $g_0(t)$. The first one lies on the border between the incoherent and the stationary state and is denoted by **II**, while the second region exists within the stationary area and is denoted by **III**. Figure 2(b) shows the corresponding snapshot representations of the amplitude of the electric field (left), the spatiotemporal evolution of the local curvature (middle), and that of the local order parameter (right). Note that the local curvature has been normalized to its maximum value [24].

Moving from points **I** to **IV**, the system goes from the incoherent state to the stationary one through a wavelike spatial structure (point **II**) and an almost fully stationary state (point **III**). In the incoherent state the lasers are desynchronized both in amplitude and in phase, which is depicted in the local curvature and the local order parameter. With increase of the coupling range R , the temporal oscillations of the lasers tend to become closer in amplitude. This is reflected in the smooth wavelike structure of the amplitude of the electric fields and the discrete Laplacian which holds a value close to zero. The corresponding phase oscillations are less coherent and this is evident by the blue areas in the order parameter spatiotemporal plot.

Before entering the fully stationary state (**IV**) the systems undergoes another interesting region where $g_0(t)$ is close, but less than one because of a deviation from the stationary state of two lasers (left panel of **III**), which holds for both the amplitude (middle) and the phase (right). In coupled systems, the phenomenon where one or more oscillators exhibit large amplitude oscillations whereas the rest are stationary, is called localized breather and has been intensively investigated in the past [28,29].

For finite coupling phase C_p , the situation is much more complicated. By plotting the temporal mean of $g_0(t)$ in the (C_p, k) plane [Figs. 3(a), 3(c) and 3(e)] as well as in the (C_p, R) plane [Figs. 3(b), 3(d), and 3(f)] for various values of the coupling strength k and the coupling range R , we can identify the existence of many patterns, among which chimera

states, which we have marked with roman letters. Each chimera state is characterized by its multiplicity, i.e., the number of the (in)coherent regions also known as number of chimera clusters. Single chimeras (**I**), as well as chimeras with two (**II**), six (**III**), and nine heads (**IV**) are observed. Moreover, localized oscillations and waves similar to those of Fig. 2 are also found (not shown). Finally, “turbulent” chimeras [21] where the position of the (in)coherent regions changes in time and $g_0(t)$ oscillates irregularly complete the picture of the observed patterns (**V**).

More specifically, for nonlocal range coupling $R > 10$ and coupling strength $k > 0.05$, we can distinguish different regions in terms of the coupling phase value. Below those two values the interaction is so weak that each laser behaves like an uncoupled one (see Fig. 3, lower left corners of all panels). Around the region $C_p \approx 0$ and the region $C_p \approx \pi$ the case of full synchronization is most prominent, where $\mathcal{E}_i = \mathcal{E}_j$ holds for all lasers. The opposite situation of full asynchrony

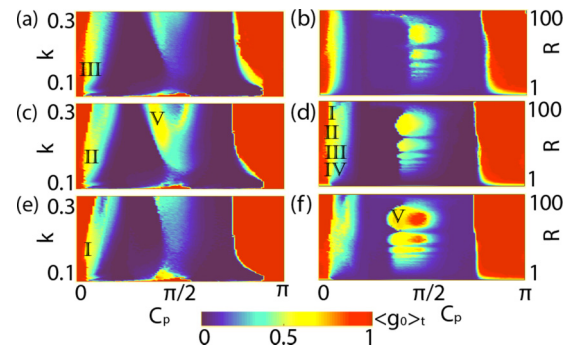


FIG. 3. Dependence of the temporal mean $\langle g_0(t) \rangle$ on parameters k and C_p for different values of nonlocal coupling range: (a) $R = 40$, (c) $R = 64$, and (e) $R = 88$. Dependence on parameters R and C_p of the temporal mean $\langle g_0(t) \rangle$ for different values of the coupling strength: (b) $k = 0.075$, (d) $k = 0.15$, and (f) $k = 0.225$. Other parameters: $T = 392$, $p = 0.23$, and $a = 2.5$.

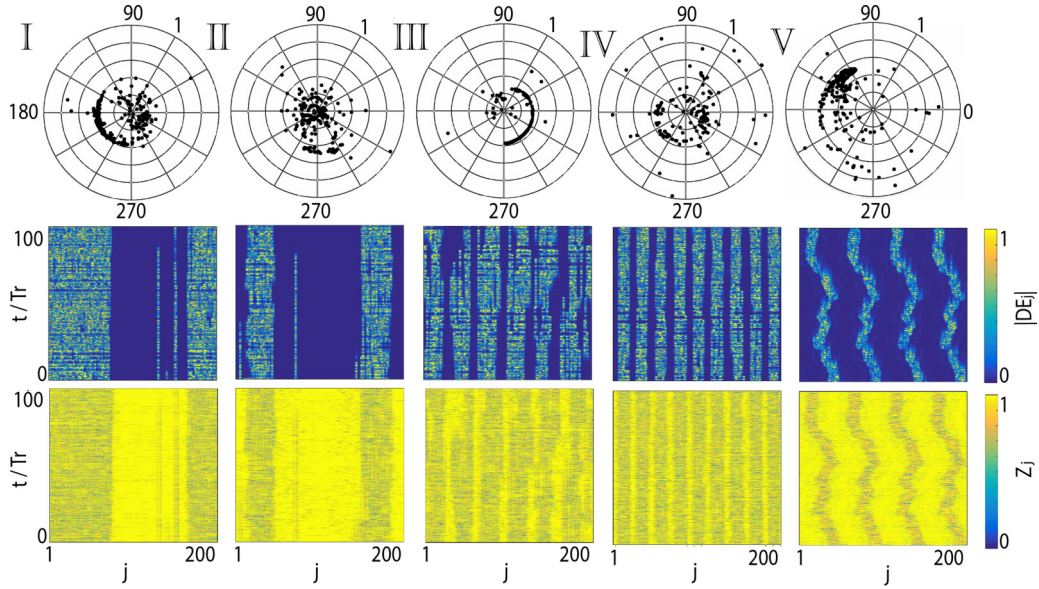


FIG. 4. The electric field in the complex unit circle (top), spatio-temporal evolution of the local curvature (middle), and spatio-temporal evolution of the local order parameter (bottom) for different coupling ranges and phases: **(I)** $R = 88, C_p = 0.1\pi, k = 0.15$; **(II)** $R = 64, C_p = 0.06\pi, k = 0.15$; **(III)** $R = 40, C_p = 0.1\pi, k = 0.15$; **(IV)** $R = 27, C_p = 0.1\pi, k = 0.15$; and **(V)** $R = 64, C_p = 0.4\pi, k = 0.225$. Other parameters: $T = 392, p = 0.23$, and $a = 2.5$.

where both amplitude and phase exhibit incoherent behavior appears around the regions $C_p \approx \pi/4$ and $C_p \approx 3\pi/4$. On the boundary between full synchronization and asynchrony lies a small area where the chimeras arise.

Figure 4 shows typical snapshots of multiclustered chimera states of the electric field in the complex unit circle (top panel), the spatiotemporal evolution of the local curvature (middle panel) and the spatiotemporal evolution of the local order parameter (bottom panel) for points **I–IV**. We observe that the decrease of R yields additional chimera heads both in amplitude and in phase. Finally, around the region where $C_p \approx \pi/2$ turbulent chimeras appear (Fig. 4, **V**).

V. CONCLUSIONS

In conclusion, multiclustered chimera states have been obtained and characterized in large arrays of semiconductor class B lasers with nonlocal interactions. The observed chimeras display the coherence and incoherence patterns in both the amplitude and phase of the electric field and can be both stationary or “turbulent,” where the size and position of the (in)coherent clusters vary in time. In addition, other spatiotemporal dynamics including wavelike spatial structures and spatially localized oscillations (breathers) are possible.

The crucial parameters for the collective behavior are the complex coupling strength and the nonlocal coupling range. The latter is responsible for the multiplicity of the (in)coherent domains of the obtained chimeras which has been observed neither for local nor for global coupling. By applying recently presented measures for spatial coherence we have identified and classified the emerging dynamics in the relevant parameter spaces. Our study addresses the effect of nonlocal coupling in large laser arrays for the first time, providing a direction for various technological applications. By considering the proposed setups for the nonlocal coupling scheme, our results can prove useful for further experimental investigations. For future studies it would be worthwhile to explore the influence of noise and anisotropy in the laser pump power.

ACKNOWLEDGMENTS

This work was partially supported by the Ministry of Education and Science of the Russian Federation in the framework of the Increase Competitiveness Program of NUST “MISiS” (Grant No. K2-2015-007) and the European Commission under project NHQWAVE (MSCA-RISE 691209). P.H. acknowledges support by Deutsche Forschungsgemeinschaft in the framework of SFB 910. Moreover, the authors thank V. Kovanis for fruitful discussions.

-
- [1] G. Kozyreff, A. G. Vladimirov, and P. Mandel, *Phys. Rev. Lett.* **85**, 3809 (2000).
 [2] R. A. Oliva and S. H. Strogatz, *Int. J. Bifurcat. Chaos* **11**, 2359 (2001).
 [3] A. Uchida, Y. Liu, I. Fischer, P. Davis, and T. Aida, *Phys. Rev. A* **64**, 023801 (2001).

- [4] T. Dahms, J. Lehnert, and E. Schöll, *Phys. Rev. E* **86**, 016202 (2012).
 [5] M. C. Soriano, J. Garca-Ojalvo, C. R. Mirasso, and I. Fischer, *Rev. Mod. Phys.* **85**, 421 (2013).
 [6] G. Lythe, T. Erneux, A. Gavrielides, and V. Kovanis, *Phys. Rev. A* **55**, 4443 (1997).

- [7] L. M. Pecora, F. Sorrentino, A. M. Hagerstrom, T. E. Murphy, and R. Roy, *Nat. Commun.* **5**, 4079 (2014).
- [8] P. M. Alsing, V. Kovanis, A. Gavrielides, and T. Erneux, *Phys. Rev. A* **53**, 4429 (1996).
- [9] G. Kozyreff, A. G. Vladimirov, and P. Mandel, *Phys. Rev. E* **64**, 016613 (2001).
- [10] F. Böhm, A. Zakharova, E. Schöll, and K. Lüdge, *Phys. Rev. E* **91**, 040901(R) (2015).
- [11] W. J. Rappel, *Phys. Rev. E* **49**, 2750 (1994).
- [12] M. Silber, L. Fabiny, and K. Wiesenfeld, *Opt. Soc. Am. B* **10**, 1121 (1993).
- [13] N. Blackbeard, S. Wicczorek, H. Erzgräber, and P. S. Dutta, *Physica D (Amsterdam)* **286**, 43 (2014).
- [14] H. G. Winful and L. Rahman, *Phys. Rev. Lett.* **65**, 1575 (1990).
- [15] S. S. Wang and H. G. Winful, *Appl. Phys. Lett.* **52**, 1774 (1988).
- [16] Y. Kuramoto and D. Battogtokh, *Nonlinear Phenom. Complex Syst.* **5**, 380 (2002).
- [17] M. J. Pannaggio and D. Abrams, *Nonlinearity* **28**, R67 (2015).
- [18] L. Larger, B. Penkovsky, and Y. Maistrenko, *Phys. Rev. Lett.* **111**, 054103 (2013).
- [19] L. Larger, B. Penkovsky, and Y. Maistrenko, *Nat. Commun.* **6**, 7752 (2015).
- [20] A. Röhm, F. Böhm, and K. Lüdge, *Phys. Rev. E* **94**, 042204 (2016).
- [21] J. Shena, J. Hizanidis, V. Kovanis, and G. P. Tsironis, *Sci. Rep.* **7**, 42116 (2017).
- [22] M. Nixon, M. Friedman, E. Ronen, A. A. Friesem, N. Davidson, and I. Kanter, *Phys. Rev. Lett.* **108**, 214101 (2012).
- [23] M. Nixon, E. Ronen, A. A. Friesem, and N. Davidson, *Phys. Rev. Lett.* **110**, 184102 (2013).
- [24] F. P. Kemeth, S. W. Haugland, L. Schmidt, I. G. Kevrekidis, and K. Krischer, *Chaos* **26**, 094815 (2016).
- [25] J. Katz, E. Kapon, C. Lindsey, S. Margalit, and A. Yariv, *Appl. Opt.* **23**, 2231 (1984).
- [26] I. Omelchenko, O. E. Omelchenko, P. Hövel, and E. Schöll, *Phys. Rev. Lett.* **110**, 224101 (2013).
- [27] N. E. Kouvaris, R. J. Requejo, J. Hizanidis, and A. D. Guilera, *Chaos* **26**, 123108 (2016).
- [28] R. S. Mackay and S. Aubry, *Nonlinearity* **7**, 1623 (1994).
- [29] D. Chen, S. Aubry, and G. P. Tsironis, *Phys. Rev. Lett.* **77**, 4776 (1996).